American Journal of Pathology, Vol. 166, No. 4, April 2005

Musculoskeletal Pathology

Interleukin-15 Administration Improves Diaphragm Muscle Pathology and Function in Dystrophic *mdx* Mice

Leah J. Harcourt, Anna Greer Holmes, Paul Gregorevic, Jonathan D. Schertzer, Nicole Stupka, David R. Plant, and Gordon S. Lynch

From the Department of Physiology, University of Melbourne, Victoria, Australia

Interleukin (IL)-15, a cytokine expressed in skeletal muscle, has been shown to have muscle anabolic effects *in vitro* and to slow muscle wasting in rats with cancer cachexia. Whether IL-15 has therapeutic potential for diseases such as Duchenne muscular dystrophy (DMD) is unknown. We examined whether IL-15 administration could ameliorate the dystrophic pathology in the diaphragm muscle of the *mdx* mouse, an animal model for DMD. Four weeks of IL-15 treatment improved diaphragm strength, a highly significant finding because respiratory function is a mortality predictor in DMD. Enhanced diaphragm function was associated with increased muscle fiber cross-sectional area and decreased collagen infiltration. IL-15 administration was not associated with changes in T-cell populations or alterations in specific components of the ubiquitin proteasome pathway. To determine the effects of IL-15 on myofiber regeneration, muscles of IL-15-treated and untreated wild-type mice were injured myotoxically, and their functional recovery was assessed. IL-15 had a mild anabolic effect, increasing fiber cross-sectional area after 2 and 6 days but not after 10 days. Our findings demonstrate that IL-15 administration improves the pathophysiology of dystrophic muscle and highlight a possible therapeutic role for IL-15 in the treatment of neuromuscular disorders especially in which muscle wasting is indicated. *(Am J Pathol 2005, 166:1131–1141)*

Duchenne muscular dystrophy (DMD) is a severe X chromosome-linked disorder caused by mutations in the dystrophin gene, resulting in a lack of dystrophin expression that compromises the structural integrity of the muscle fiber membrane and renders muscles more susceptible to contraction-mediated injury and degeneration.[1–7] As a consequence, dystrophic muscle fibers continually undergo degeneration only to be replaced by regenerating fibers with the same genetic deficiency and injury susceptibility. The *mdx* mouse, a commonly used animal model for DMD, carries a mutation in the dystrophin gene and lacks the native protein similar to the human condition, but exhibits a more benign pathological phenotype. The diaphragm muscles of *mdx* mice show progressive structural and functional deterioration consistent with DMD, whereas limb muscles exhibit a relatively mild pathology for much of the life span.[7–11] The diaphragm could therefore provide a more sensitive screen for drug efficacy.

Many therapeutic trials have been undertaken with the purpose of ameliorating (or potentially curing) the muscular dystrophies. The aims of any approach for treating muscular dystrophy are to attenuate muscle wasting by maintaining or increasing muscle mass, responses that would translate to either a preservation or an increase in muscle strength. The therapeutic approaches that have been attempted for DMD or animal models of muscular dystrophy, especially the *mdx* mouse, include the use of anabolic agents, corticosteroids, Ca^{2+} channel blockers, growth hormone secretion modulators, antioxidants, amino acids, immunosuppressives, and vitamins.[12] Calcium channel blockers, growth hormone inhibitors, and vitamin E, all proved unsuccessful, ie, they provided no beneficial effects.[13] Several trials with corticosteroids, such as prednisone and/or deflazacort, have been shown to provide some level of improvement of the dystrophic pathology, evidenced by small but significant improvements in muscle strength.[14] However, not all trials were conclusive and long-term use of glucocorticoids has been accompanied by side effects including weight gain, growth retardation, and fluid retention.[12,15] Rather than increasing muscle size and strength, the use of corticosteroids maintains or reduces muscle fiber size. Con-

Supported by research grants from the Muscular Dystrophy Association.

Accepted for publication December 7, 2004.

Address reprint requests to Gordon S. Lynch, Ph.D., Department of Physiology, University of Melbourne, Victoria, Australia, 3010. E-mail: gsl@unimelb.edu.au.

versely, administration of growth factors (eg, insulin-like growth factor-I) and other anabolic agents (eg, β-adrenoceptor agonists) aims to enhance muscle size and strength.[16–19] Although improvements in muscle size and strength have been reported in *mdx* mice after administration of these compounds, their clinical application for dystrophy and other muscle wasting disorders has been limited because of concerns about potential cardiovascular and/or cancer-related side effects.[20,21] Recent advances have identified a diversity of possible therapeutic approaches, from pharmacological treatments, including the use of myostatin antibodies,[22,23] gene therapies (exon-skipping and adeno-associated viruses), and cell therapy with different types of newly identified stem cells.[13,24]

Although gene therapies are expected to eventually provide a cure for neuromuscular pathologies, existing methodologies have yet to transition into human clinical trials in which any efficacy can be expected. There are also concerns regarding safety of gene delivery methods.[25] Until genetic therapies are optimized, it is essential that other interventions be evaluated for treating the symptoms of these muscle diseases to enhance patient quality of life. Such therapies primarily focus on either slowing the loss of muscle to preserve function or increasing muscle mass to improve function.

One therapeutic approach that has not been tested rigorously is treatment with the growth factor, interleukin (IL)-15. IL-15 is a cytokine that has the ability to stimulate T-cell proliferation and enhance natural killer activity.[26] IL-15 is expressed in skeletal muscle and studies *in vitro* have shown it to increase contractile proteins in differentiated myocytes,[27–30] and increase myogenic differentiation in conditions in which insulin-like growth factor-I concentrations are lower.[29] Such is the case in muscular dystrophy, in which the circulating levels of insulin-like growth factor-I are depressed and muscle regeneration is compromised.[31] The reported anabolic actions of IL-15 makes it attractive as a treatment strategy for muscle wasting, including that associated with DMD. The clinical potential of IL-15 treatment was evident from a study that showed it could attenuate muscle wasting in a rat model of cancer cachexia, primarily through decreasing the rate of skeletal muscle proteolysis via an inhibition of the genes associated with the ATP-ubiquitin-dependent proteolytic pathway.[32]

IL-15 is still one of the most understudied of all skeletal muscle growth factors and whether it has clinical application for muscular dystrophy is unknown. We tested the hypothesis that IL-15 administration would improve diaphragm muscle function in *mdx* mice by ameliorating the dystrophic pathology. To elucidate one of the possible underlying mechanisms of IL-15 treatment, we also examined whether IL-15 treatment would hasten muscle regeneration after myotoxic injury, and tested the hypothesis that functional recovery would be improved through enhanced muscle fiber growth.

Materials and Methods

All experiments were approved by the Animal Experimentation Ethics Committee of The University of Melbourne and complied with the Code of Conduct for the Care and Use of Animals as specified by the National Health and Medical Research Council of Australia. Male, 8-week-old wild-type C57BL/10 ScSn and C57BL/10ScSn-*mdx*/J dystrophic (*mdx*) mice were randomly assigned to either untreated ($n = 8$) or IL-15-treated groups ($n = 8$). The mice were housed in the Biological Research Facility at the University of Melbourne and maintained on a 12-hour light/12-hour dark cycle, with standard mouse chow and water provided *ad libitum*.

IL-15 Administration

Stock human recombinant IL-15 was kindly provided by Amgen Inc. (Thousand Oaks, CA). Previous studies have shown that human IL-15 is similar in homology to mouse IL-15 and appropriate for use in a murine model.[33] IL-15 was dissolved in sterile isotonic saline at a concentration of 3.79 mg/ml and loaded into miniosmotic pumps (model 1002; Alzet, Cupertino, CA). Treated mice were implanted with a pump that had been partially dipped in paraffin wax to achieve a pumping rate of ~0.125 μl/hour (3 μl/day) for 28 days.[34] Treated mice received 10 μg of IL-15 per day, approximately equivalent to 0.5 mg/kg/day for a 25 g mouse. Untreated mice did not receive a sham pump because we have shown previously that implantation of the pump alone, or delivery of saline vehicle, does not affect muscle structure or function.[19] Pumps were surgically implanted into anesthetized mice (70 mg/kg^{-1}, i.p., sodium pentobarbitone; Rhone Merieux, Pinkenba QLD, Australia) so that there was no response to tactile stimulation. An incision was made in the skin in the middle of the spinal curvature and a subcutaneous pocket created by blunt dissection with surgical scissors. The pumps were inserted with the flow regulator cap orientated distally and the incision closed with surgical clips. Body mass was monitored daily to ensure that no mice exhibited adverse effects to either the surgical procedure or IL-15 treatment.

Assessment of Muscle Function

At the completion of the 4-week treatment period, mice were anesthetized deeply with sodium pentobarbitone with supplemental doses administered as necessary to prevent any response to tactile stimulation. The entire diaphragm and surrounding ribcage were carefully excised and placed into a dish containing oxygenated Ringer solution (NaCl, 137 mmol/L; $NaHCO_3$, 24 mmol/L; D-glucose, 11 mmol/L; KCl, 5 mmol/L; $CaCl_2$, 2 mmol/L; $NaH_2PO_4H_2O$, 1 mmol/L; $MgSO_4.7H_2O$, 487 μmol/L; D-tubocurarine chloride, 293 μmol/L). Diaphragm strips composed of longitudinally arranged full-length muscle fibers were tied firmly with braided surgical silk (6/0; Pearsalls Sutures, Somerset, UK) at the central tendon at one end, and sutured through a portion of rib attached to the distal end of the strip at the other end. Mice were killed as a consequence of diaphragm and heart excision while anesthetized.

The procedures for evaluating the functional properties of diaphragm muscle strips *in vitro* have been described

by us in detail previously.[7,18] Briefly, the diaphragm strips were transferred to a custom built Plexiglas bath which was filled with oxygenated Ringer solution, thermostatically maintained at 25°C for optimal oxygen diffusion. The muscles were aligned horizontally and tied directly between a fixed pin and a dual-mode force transducer-servomotor (300B-LR; Aurora Scientific, Aurora, Ontario, Canada). Two platinum plate electrodes were positioned in the organ bath so as to flank the length of the muscle preparation. Muscles were field-stimulated by supramaximal square wave pulses (0.2 ms duration), that were amplified (EP500B power amplifier; Audio Assemblers, Campbellfield, Victoria, Australia) to increase and sustain current intensity to a sufficient level to produce a maximum isometric tetanic contraction.

All stimulation parameters and contractile responses were controlled and measured using custom built applications (D.R. Stom Inc., Ann Arbor MI) of LabView software (National Instruments, Austin, TX) driving a personal computer with onboard controller (PCI-MIO-16XE-10, National Instruments) interfaced with the transducer-servomotor control/feedback hardware (Aurora Scientific). Optimum muscle length (L_o) and stimulation voltage were determined from micromanipulation of muscle length to produce maximum isometric twitch force (P_t). Optimum fiber length (L_f) was equal to L_o based on the alignment of the fibers in the diaphragm preparation as determined previously.[7] Maximum isometric tetanic force (P_o) was determined from the plateau of the frequency-force relationship after successive stimulations at 5 to 150 Hz for 450 ms, with 2 minutes rest between stimuli.

After determination of the frequency-force relationship, muscles were subjected to a 4-minute repeated stimulation protocol to examine muscle fatigue. Muscles at L_o were maximally stimulated once every 5 seconds for the duration of the 4-minute fatigue protocol. After a 5-minute rest interval (of no stimulation), the diaphragm muscle strip was maximally stimulated once (at 5, 10, and 15 minutes) to determine the recovery P_o. After functional testing, the muscle was removed from the bath, trimmed of tendon and any adhering nonmuscle tissue, blotted once on filter paper, and weighed on an analytical balance. The muscles were arranged at L_o on a small piece of aluminum foil, embedded in O.C.T compound (4583; Tissue Tek, Sakura, CA), snap-frozen in thawing isopentane and stored at −80°C. Because the width of individual diaphragm preparations (and hence the total number of fibers tested) varies based on the discretion of the individual performing the dissections, comparisons of absolute P_t and P_o values are not valid, and all data must be normalized with respect to the length and width (and therefore mass) of individual muscles. Muscle mass, L_f and P_o were used to calculate specific force (sP_o, or force normalized per total muscle fiber cross-sectional area, kN/m^2) taking into account muscle density (1.06 mg/mm^3) as described elsewhere.[7,18] The value for muscle density is resistant to variation beyond the third decimal place and from variations in connective tissue, fat, and water composition.[35]

Morphological Properties

Sections (8 μm thick) were cut from the middle portion of the diaphragm muscle strips on a cryostat (IEC, Needham Heights, MA) at −20°C and then placed on either uncovered glass or silane-covered slides for immunohistochemistry. One section was stained with hematoxylin and eosin (H&E) for determination of general muscle architecture and the other with Van Gieson's stain for collagen localization. The remaining slides were used for immunohistochemistry and air-dried overnight, then stored at −80°C until used.

Digitised images (12-bit gray scale) of muscle sections were acquired using an upright microscope (BH-2; Olympus, Tokyo, Japan) and camera (Spot model 1.3.0; Diagnostic Instruments, Sterling Heights MI), driven by Spot diagnostic software (v2.1, Diagnostic Instruments). Image files were analyzed with Image Pro (v4.0; Media Cybernetics, Silver Spring, MD). The cross-sectional area (CSA) of diaphragm muscle fibers was calculated by determination of the circumference of ~100 adjacent cells from every muscle section examined. Although it is not possible to know whether the concentration of collagen is uniform throughout the Van Gieson-stained regions, this measurement allows assessment of the area of collagen infiltration within a muscle cross-section and provides important structure-function information especially for diaphragm muscle strips.

Immunohistochemistry

Tissue preparation and immunohistochemistry were performed modified by the protocol described previously.[36] Sections were air-dried for overnight and stored at −80°C until required for use. Slides were fixed in ice-cold acetone for 15 minutes, washed in Tris-buffered saline (TBS), then placed in 1.5% H_2O_2 (diluted in TBS) to block endogenous peroxidase activity for 10 minutes. Sections were blocked with normal goat serum for 15 minutes to prevent nonspecific binding and the relevant primary and secondary antibodies were applied. The slides were developed using 3-amino-9-ethyl carbazole (AEC, K3469; DAKO, Sydney, Australia) and allowed to react for 2 minutes. Sections were counterstained with hematoxylin to emphasize the architecture of the muscle. The analysis of each diaphragm section was blinded to the investigator.

Macrophages

Positive and negative controls were used for each run using sections of mouse spleen to confirm that the technique was working correctly. Sections were processed for immunohistochemistry with rat anti-mouse F4/80 (MCA497R, diluted 1:60; Serotec, Oxford, UK), which recognizes antigens specific for macrophages, for 2 hours. The sections were washed in TBS and incubated with secondary goat anti-rat antibody STAR72 (diluted 1:50, Serotec) for 30 minutes. Sections were washed three times with TBS and the antibody-antigen complex was revealed with an AEC and substrate-chromogen kit (K3469, DAKO). Macrophage density was examined by

counting the number of labeled macrophages in two fields of each diaphragm strip blinded to the investigator and expressed as macrophages per mm^2.

T Cells ($CD4^+$ and $CD8^+$)

T cells were quantified as an indication of inflammation after IL-15 administration. It has been demonstrated previously that T-cell numbers are associated with increased pathology in the muscles of *mdx* mice[37] and that T cells may play a role in the onset of the fibrotic events that undermine the ability of dystrophic muscles to regenerate.[38] Positive and negative controls were used for each run using sections of mouse spleen and thymus which both contain large T-cell populations. Sections were processed for immunohistochemistry with purified rat anti-mouse CD4 (550280; Biosciences, Sydney, Australia) and purified rat anti-mouse CD8a (550281, Biosciences), diluted 1:30 in normal goat serum. The sections were incubated with the polyclonal rabbit anti-rat secondary antibody (diluted 1:200, E 0468; DAKO). streptavidin was applied (diluted 1:400, P 0397; DAKO) for 30 minutes. Sections were washed and the antibody-antigen complex was revealed. T-cell density was examined by counting the number of labeled $CD4^+$ or $CD8^+$ cells in each diaphragm strip (blinded to the investigator) and expressed as T-cell number per mm^2.

IL-15

To confirm successful delivery of IL-15 to the diaphragm muscle of treated animals, IL-15 levels were determined via immunohistochemistry. Positive and negative controls were used each run that included slides smeared with hu-IL-15 protein as well as sections of diaphragm muscles from treated *mdx* mice. Positive control sections were reacted with M112 antibody (kindly provided by Genmab, Utrecht, The Netherlands), which was diluted 1:50; as well as biotinylated mouse immunoglobulin, normal mouse serum (X0910, DAKO), and diluent for biotinylation (S0809, DAKO). Half of the negative controls were incubated with normal mouse serum and the other half with biotinylated mouse immunoglobulin, normal mouse serum, and diluent. Diaphragm muscle sections from untreated and IL-15-treated mice that were reacted with the secondary antibody only, did not stain positive. The sections were washed in TBS and incubated with Vectastain ABC kit (PK-6100; Vector Laboratories, Burlingame, CA) for 1 hour. Each section was then washed three times with TBS and the IL-15 was revealed with an AEC and substrate-chromogen kit. IL-15 levels were quantified by calculating the proportion of the muscle section that reacted with the IL-15 antibody, using the image analysis software described previously.

Determination of Myosin Heavy Chain Composition within Diaphragm Muscles

Myosin heavy chain isoform composition was determined from homogenized muscle samples from all treatment groups. A 9% acrylamide-bis (50:1) separating gel was poured into the 1.0-mm-thick gel casting cassette (In-Vitrogen Australia Pty., Ltd., Mt. Waverly, Victoria, Australia), and left to set overnight. A 4% acrylamide-bis (50:1) stacking gel was poured on top of the separating gel and set for ~3 hours with a 10-well comb.

Frozen diaphragm muscle samples were thawed, tendon removed, and then weighed, diluted in a 1:30 solution of homogenizing buffer (50 mmol/L KCl, 10 mmol/L KH_2PO_4, 2 mmol/L $MgCl_2.6H_2O$, 0.5 mmol/L ethylenediamine tetraacetic acid, 2 mmol/L DTT), and homogenized using a glass homogenizer. Samples were then transferred to Eppendorf tubes, and centrifuged at 1000 $\times$ *g* for 10 minutes at 5°C. The pellet was resuspended in 1:30 wet weight:volume using homogenizing buffer (60 mmol/L KCl, 130 mmol/L imidazole, 2 mmol/L $MgCl_2.6H_2O$ 1 mmol/L DTT). A Bradford protein assay was used for protein content determination on all muscle samples. The samples were assayed in triplicate in a spectrophotometer (U-2000; Hitachi, Tokyo, Japan). Sample preparations were made up using the homogenate, storage buffer (60 mmol/L KCl, 130 mmol/L imidazole, 2 mmol/L $MgCl_2.6H_2O$, 1 mmol/L DTT) and sample buffer (1% bromophenol blue, 5.5 mol/L glycerol, 275 mmol/LM sodium dodecyl sulfate, 250 mmol/L Tris-HCl, 60 mmol/L DTT) to load 1 μg of protein per well (12 μl) for each sample. Samples were boiled for 2 minutes at 100°C and vortexed before being loaded onto the gel. Five μl of a prestained protein standard was loaded in each gel. The upper running buffer (10 mmol/L sodium dodecyl sulfate, 450 mmol/L glycine, 300 mmol/L Tris base, 10 mmol/L 2-mercaptoethanol) and the lower running buffer (1.7 mmol/L sodium dodecyl sulfate, 75 mmol/L glycine, 50 mmol/L Tris base, 10 mmol/L 2 mercaptoethanol) were made fresh for each run. The gels were run at 110 V at 4°C for 16 hours. Protein bands were visualized using the In-Vitrogen Silver Stain kit (LC6100). The gels were then scanned and band densities analyzed using the image analysis software described previously.

Determination of Specific Components of the Ubiquitin Proteosome Pathway in Diaphragm Muscles

Total RNA from diaphragm muscles was isolated using a commercially available kit according to the manufacturer's instructions (no. 74704; Qiagen, Valencia, CA). RNA concentration was determined by UV absorption at 260 nm, and the samples were stored at −80°C. Analysis of mRNA levels for ubiquitin and the ubiquitin-conjugating enzyme E214k/HR6B were performed using gene-specific primers. Ubiquitin used primers 5′-CCAATGGCGGTTAATGACCTT-3′ and 5′-TTTCGATGGGGCTTGAGGATT-3′, resulting in a 141-bp product. E214k/HR6B used primers 5′-GCCCCATCTGAAAACAACAT-3′ and 5′-CGGTTCATCCAGCAGAGACT-3′, resulting in a 270-bp fragment. 18S was used as a loading control and the primers were 5′-AAACGGCTACCACATCCAAG-3′ and 5′-CCCTCTTAATCATGGCCTCA-3′, resulting in a 479-bp product. Semi-quantitative reverse transcriptase (RT)-polymerase chain reaction (PCR) was performed on 200 ng of total RNA.

Reverse transcriptase and polymerase chain reactions were performed using a commercially available kit according to the manufacturer's instructions (no. 74704, Qiagen). A standard RT-PCR protocol was used and consisted of 30 minutes at 50°C, 15 minutes at 95°C, and repeated cycles of denaturation (94°C, 45 seconds), annealing (various temperatures, 45 seconds), and extension (72°C, 45 seconds). The annealing temperatures were 57°C for E214k/HR6B, 50°C for ubiquitin, and 50°C for 18S. The RT-PCR products were electrophoresed on 2% agarose gels in Tris-acetate, ethylene-diaminetetra-acetic acid buffer and photographed under UV light after staining with ethidium bromide. We have reported RT-PCR after varying the number of cycles for each target mRNA to demonstrate that the amplified signal was on the linear portion of a semilog plot of the yield, expressed as a function of the number of cycles.

Crude muscle homogenates were prepared by diluting diaphragm muscle 1:10 wt:vol in ice-cold homogenization buffer and mechanical homogenization, as described previously.[39] Total muscle protein was determined by Bradford assay. Crude muscle homogenate proteins were separated by sodium dodecyl sulfate-polyacrylamide gel electrophoresis (4 to 12% gradient gels) and transferred to polyvinylidene membranes. Equal protein loading was validated by Ponceau red staining. Membranes were blocked for 1 hour with 5% nonfat milk and 2.5% bovine serum albumin. Immunoblotting was performed for 1 hour at room temperature using a mouse monoclonal antibody that detects ubiquitin and ubiquitinated proteins (no. sc-8017; Santa Cruz Biotechnology, Santa Cruz, CA). After adequate washes in phosphate-buffered saline plus 0.1% Tween, specific proteins were detected with a mouse horseradish peroxidase-conjugated secondary antibody and enhanced chemiluminescence, as described previously.[39] Gels were digitized and relative protein levels were determined by scanning densitometry. Values ($n = 3$ for each condition) were expressed as a percentage of the optical density for diaphragm muscles from untreated C57/BL10 mice.

Effect of IL-15 Administration on Muscle Fiber Regeneration after Myotoxic Injury

An additional group of 8-week-old male C57BL/10 ScSn wild-type mice were used to assess the effect of IL-15 administration on the rate of muscle repair after myotoxic injury. In these experiments, the extensor digitorum longus (EDL) muscles were surgically exposed and injected directly with bupivacaine hydrochloride (0.5% Marcaine; Astra, North Ryde, NSW, Australia), which causes muscle fiber degeneration followed by spontaneous muscle fiber regeneration.[40] As a model for muscle injury, bupivacaine has an advantage in that its effects are muscle fiber-specific with little or no effect on the muscle's nerve and blood supply.[40,41]

Mice were anesthetized with sodium pentobarbitone (70 mg/kg, i.p.) and the EDL of the right hindlimb exposed and injected with a maximal volume (~80 to 100 μl) of bupivacaine using a 30-gauge needle. Three sites were injected, the mid belly as well as both the proximal and distal ends, to cause degeneration of as many muscle fibers as possible.[40,41] In all mice, the EDL muscle of the left hindlimb served as the uninjured control. Previous studies have demonstrated that injection of only saline vehicle does not cause significant damage or impairment to the structure or function of the muscle and was therefore deemed unnecessary.[41,42] After injection the small skin incision was closed with surgical clips.

Mice were randomly assigned to either IL-15-treated or untreated groups. The groups were further assigned to one of three subgroups for analysis at either 2, 6, or 10 days after injury and/or treatment ($n = 8$ mice per group for each time point). The IL-15-treated mice received an identical dose to that described earlier (ie, 0.5 mg/kg/day).

At 2, 6, or 10 days after injury/treatment, the mice were anesthetized and the uninjured and injured EDL muscles were surgically excised for assessment of their isometric contractile properties *in vitro* using identical procedures as described earlier. After functional assessments, the muscles were frozen and 8-μm-thick sections stained with H&E. CSAs were determined for ~100 fibers in each section.

Statistical Analyses

All values in the text and tables are reported as mean ± SEM unless indicated otherwise. Comparisons of IL-15-treated and untreated C57BL/10 and *mdx* mice and comparisons between injured and uninjured muscles from IL-15-treated and untreated C57BL/10 mice were made using a general linear model, two-factor analysis of variance. Tukey's posthoc multiple comparison procedure was used to identify differences between groups when significance was detected. Significance was accepted at $P < 0.05$.

Data for diaphragm muscle fiber CSA was first assessed for normality using a Kolmogorov-Smirnov test. The distribution of CSAs was not normal for any of the untreated C57BL/10 or *mdx* mice. In contrast, after IL-15 treatment, the distribution of CSAs was normal in the majority of muscles from C57BL/10 but not *mdx* mice. In regenerating muscles from C57BL/10 mice, the distribution of CSAs was also not normal in the majority of muscles. Because in most cases there was a significant difference in the mean and median values, CSA data in all cases are shown as box-and-whisker plots with the 95% confidence interval of the median used for assessing differences between groups. For comparisons of diaphragm muscle fiber CSA between experimental groups, values were considered different if there was no overlap between the 95% confidence interval of the median.

Results

Effect of IL-15 Administration on Diaphragm Muscle Function in mdx Mice

The specific force (sP_o) of diaphragm muscle strips from untreated *mdx* mice was ~54% lower than that for untreated C57BL/10 mice (Table 1). At the conclusion of the 4-week treatment period, there was no difference in the

Table 1. Summary of Morphometric and Functional Data for Diaphragm Muscles Examined after 4 Weeks of IL-15 Treatment in C57BL/10 and *mdx* Mice

	C57BL/10		*Mdx*	
	Untreated (n = 8)	Treated (n = 8)	Untreated (n = 8)	Treated (n = 7)
Body mass (g)	26.5 ± 1.2	25.6 ± 1.2	30.1 ± 0.8	28.4 ± 0.5
TPT (ms)	44.1 ± 1.6	42.9 ± 2.4	42.3 ± 2.7	41.5 ± 1.5
dP_t/dt (mN/ms)	4.1 ± 0.2	3.8 ± 0.4	3.5 ± 0.3	4.5 ± 0.5
½ RT (ms)	56.8 ± 4.8	53.3 ± 6.8	52.3 ± 6.0	48.1 ± 2.7
sP_o (kN/m^2)	207 ± 6	209 ± 5	111 ± 8*	140 ± 2†

TPT, time to peak twitch tension; dP_t/dt, rate of twitch force generation throughout time; ½ RT, one-half twitch relaxation time; sP_o, specific maximum isometric tetanic force.
**mdx* versus C57BL/10 ($P < 0.05$).
†Treated versus untreated ($P < 0.05$).

sP_o of diaphragm muscle strips from untreated (207 ± 6 kN/m^2) and treated C57BL/10 (209 ± 5 kN/m^2; Table 1) mice. However, the sP_o of diaphragm muscle strips from IL-15-treated *mdx* mice was ~21% greater than that from untreated *mdx* mice. Although improved significantly, sP_o remained (~32%) lower than values for wild-type mice ($P < 0.05$; Table 1). No differences were observed in time-to-peak twitch tension (TPT), one-half relaxation time of the twitch response (½ RT), or the peak rate of twitch force (dP_t/dt) in either strain or treatment groups. No differences were observed between treated and untreated groups during the 4-minute fatigue protocol or after the 15-minute recovery period in either C57BL/10 or *mdx* mice (Figure 1).

Structural and Histological Analysis of Diaphragm Muscles after IL-15 Administration

A box-and-whisker plot representing the distribution of fiber CSAs within diaphragm muscle strips for each of the experimental groups is shown in Figure 2C. Median fiber CSA in *mdx* mice (465 to 527 μm^2, n = 695 fibers, 95% confidence intervals of median) was smaller than in C57BL/10 (control) mice (664 to 708 μm^2, n = 551). Median fiber CSA was slightly higher in C57BL/10 mice after IL-15 treatment (760 to 814 μm^2, n = 514) whereas IL-15 had no effect on median fiber CSA in *mdx* mice (655 to 704 μm^2, n = 591; Figure 2C).

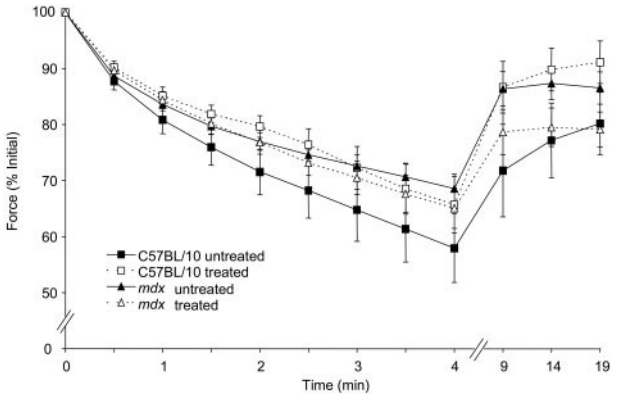

Figure 1. P_o during fatigue and recovery in diaphragm muscle strips of treated and untreated C57BL/10 and *mdx* mice. The fatigue protocol was conducted from 0 to 4 minutes, and recovery assessed at 5, 10, and 15 minutes after fatigue; n = 6 per group.

Diaphragm muscle sections from C57BL/10 mice revealed highly ordered muscle fibers with little or no collagen infiltration. In contrast, diaphragm muscles from untreated *mdx* mice had extensive muscle fiber degeneration and collagen infiltration (Figure 3). Diaphragm muscles from *mdx* mice also comprised many small caliber-regenerating fibers with centralized nuclei, characteristic of the dystrophic phenotype (Figure 2, B and C).

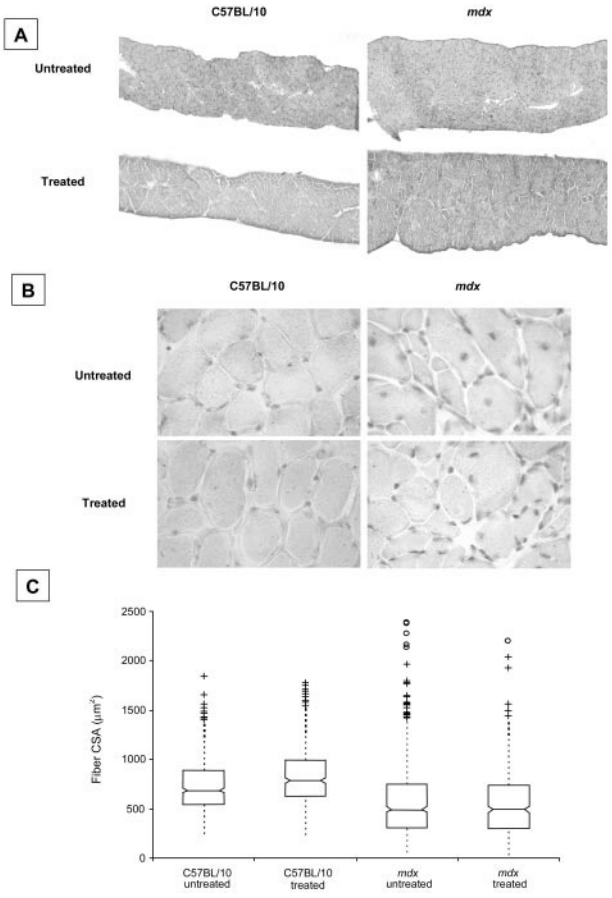

Figure 2. A: Representative cross sections of diaphragm muscles from untreated and IL-15-treated C57BL/10 and *mdx* mice stained with H&E. **B:** Higher magnification images of muscle fibers counterstained with hematoxylin to show nuclei. **C:** Box-and-whisker plots showing the distribution of fiber CSAs in diaphragm muscles. Individual outliers are depicted by the cluster of symbols in each case. Median fiber CSA was greater in IL-15-treated C57BL/10 mice but not in *mdx* mice. See text for details. Original magnifications, ×100 (**B**).

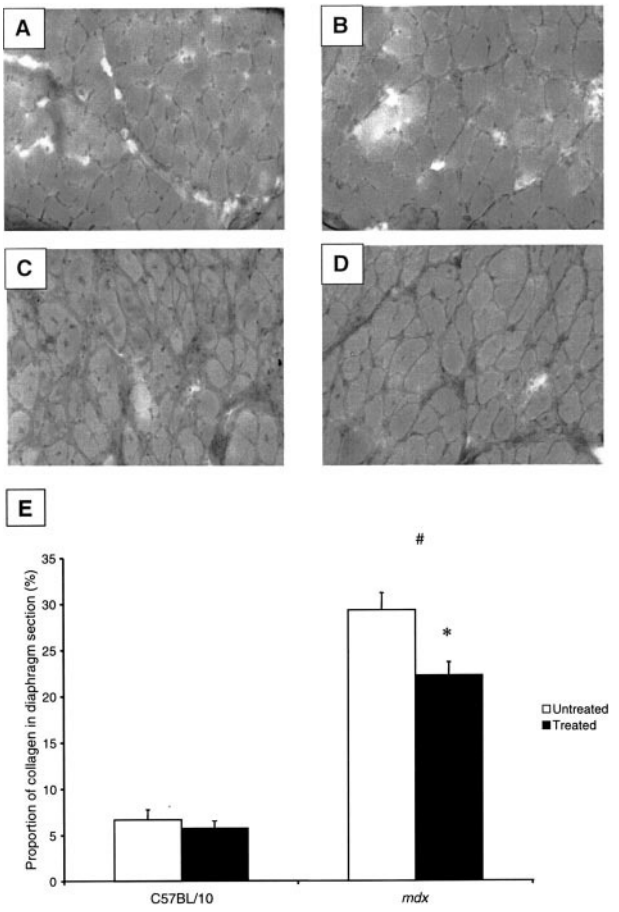

Figure 3. Van Gieson's staining of diaphragm muscles of treated and untreated C57BL/10 and *mdx* mice. **A:** Untreated C57BL/10 diaphragm strips exhibited little collagen infiltration. **B:** Treated C57BL/10 diaphragm strips also exhibited little collagen infiltration, and were not different from untreated C57BL/10 mice. **C:** Diaphragm strips from untreated *mdx* mice exhibited greater infiltration of collagen than from C57BL/10 mice. **D:** Treated *mdx* mice exhibited less collagen infiltration in the diaphragm muscle compared to untreated *mdx* mice ($P < 0.05$), but still had greater collagen infiltration than in untreated C57BL/10 mice ($P < 0.05$). **E:** Percentage infiltration of collagen in diaphragm muscle sections from treated and untreated C57BL/10 and *mdx* mice. Both treated and untreated *mdx* diaphragm muscles have greater infiltration of collagen than C57BL/10 mice (≠, $P < 0.05$). Although IL-15 treatment had no effect on collagen infiltration in the diaphragm muscles of C57BL/10 mice, treated *mdx* mice had significantly less collagen (*, $P < 0.05$).

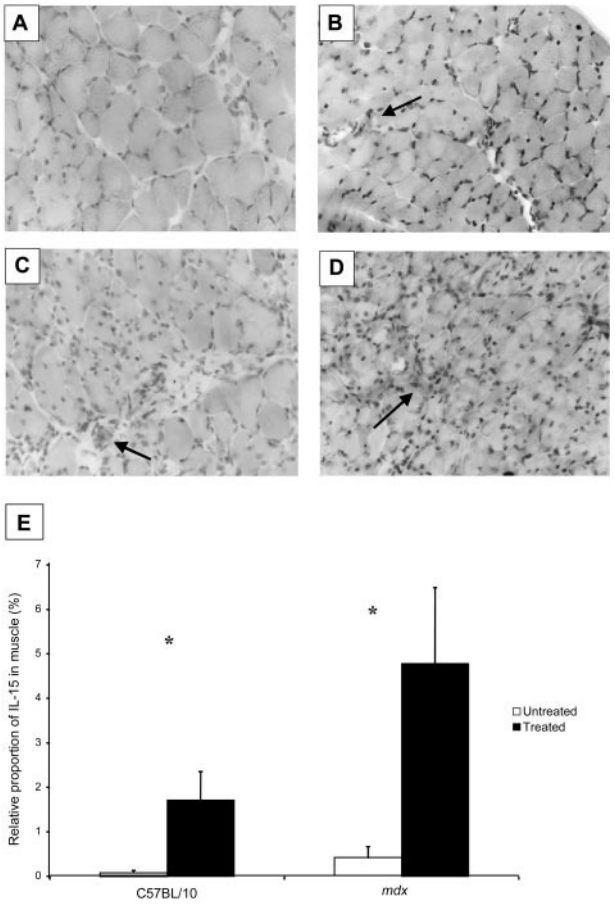

Figure 4. IL-15 reactivity of diaphragm muscles of treated and untreated C57BL/10 and *mdx* mice. **A:** IL-15 was not present in diaphragm strips from untreated C57BL/10 mice. **B:** Diaphragm muscles from treated C57BL/10 mice exhibited an ~20-fold increase in IL-15 compared with untreated C57BL/10 mice ($P < 0.05$). **C:** Untreated *mdx* mice exhibited small amounts of IL-15 in the diaphragm, usually around inflammatory cells (**arrow**). **D:** Treated *mdx* mice exhibited large amounts of IL-15 staining that was ~10-fold greater than untreated *mdx* mice ($P < 0.05$). **E:** Relative proportion (%) of IL-15 infiltration in the diaphragm muscles. Diaphragm muscles from untreated C57BL/10 and *mdx* mice exhibited little IL-15 activity, whereas treated C57BL/10 and *mdx* mice had greater activity (*, $P < 0.05$; $n = 5$ per group).

There was no difference in the proportion of fibers with central nuclei between IL-15-treated (29.3 ± 0.6%) and untreated *mdx* mice (31.6 ± 1.4%). Diaphragm muscles from *mdx* mice had greater (29.3 ± 1.9%) collagen infiltration in the muscle cross-section than muscles from untreated C57BL/10 mice (6.6 ± 1.1%; Figure 2 and Figure 3, A and D). Although IL-15 treatment did not affect collagen distribution in diaphragm muscles of C57BL/10 mice (5.8 ± 0.8%), overall collagen distribution was lower in diaphragm muscles from *mdx* mice (22.3 ± 1.4%) after IL-15 treatment ($P < 0.05$, Figure 3E).

Immunohistochemistry

Very low levels of IL-15 were present in diaphragm muscles from untreated C57BL/10 mice. However, treated C57BL/10 mice had ~20-fold greater levels of IL-15 in their diaphragm muscles ($P < 0.05$; Figure 4, B and E). Diaphragm muscles of untreated *mdx* mice exhibited some reactivity to IL-15, particularly where inflammatory cells were located. Treated *mdx* mice had ~10-fold higher IL-15 levels than untreated *mdx* mice ($P < 0.05$; Figure 4, D and E). IL-15 appeared not to be located within individual muscle fibers but in areas of inflammation and degeneration. Individual inflammatory cells reacted positively, especially in the diaphragm muscles of treated *mdx* mice (Figure 4, C and D).

Virtually no macrophages were detected in the diaphragm muscle sections from untreated or treated C57BL/10 mice. Untreated *mdx* mice had ~55-fold higher proportion of macrophages than C57BL/10 mice ($P < 0.05$; Figure 5, A to E). IL-15 treatment had no discernible effect on the macrophage population in diaphragm muscles from either C57BL/10 or *mdx* mice (Figure 5E). Similarly, IL-15 treatment had no effect on T-cell numbers in diaphragm muscles from C57BL/10 or *mdx*

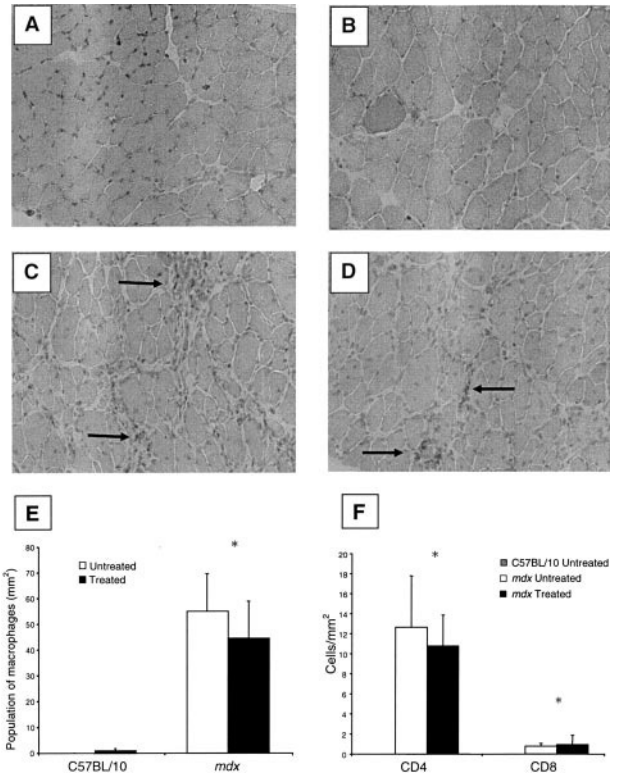

Figure 5. Immunohistochemical staining for macrophages in treated and untreated C57BL/10 and *mdx* mice diaphragm muscles. **A–D:** Diaphragm strips from untreated and treated C57BL/10 mice exhibited virtually no macrophage activity (**A**, **B**), whereas untreated and treated *mdx* mice exhibited greater macrophage populations especially in areas of muscle degeneration (**arrows**) (**C**, **D**). IL-15 treatment had no effect on macrophage population in diaphragm muscles of C57BL/10 or *mdx* mice. **E:** Population of macrophages in diaphragm strips (mm^2). Treated and untreated C57BL/10 mice had virtually no macrophages in the sections of diaphragm muscle, whereas treated and untreated *mdx* mice had a higher macrophage population (*, $P < 0.05$). There was no difference in macrophage populations in diaphragm muscle sections after IL-15 treatment in either C57BL/10 or *mdx* mice. **F:** Population of T cells ($CD4^+$ and $CD8^+$) in diaphragm muscles (mm^2). Untreated C57BL/10 mice had virtually no T cells in diaphragm muscle sections whereas T-cell ($CD4^+$ and $CD8^+$) numbers were increased in muscles from *mdx* mice (*, $P < 0.05$). IL-15 treatment did not affect T-cell numbers.

mice (Figure 5F). IL-15 treatment also had no effect on the proportions of MyHC isoforms within diaphragm muscles of C57BL/10 and *mdx* mice (Figure 6, A and B).

Ubiquitin and Ubiquitin-Conjugating Enzyme

No differences were observed in gene expression for ubiquitin and the ubiquitin-conjugating enzyme (E214K/HR6B) in diaphragm muscles from C57BL/10 and *mdx* mice and this was not altered by IL-15 treatment (Figure 7A). Similarly, ubiquitin protein levels were not different between C57BL/10 and *mdx* mice, and were not altered by IL-15 treatment (Figure 7, B and C). However, levels of ubiquitinated proteins were ~200% higher in diaphragm muscles of *mdx* compared with C57BL/10 mice. IL-15 treatment did not alter the levels of ubiquitinated proteins (Figure 7, B and C).

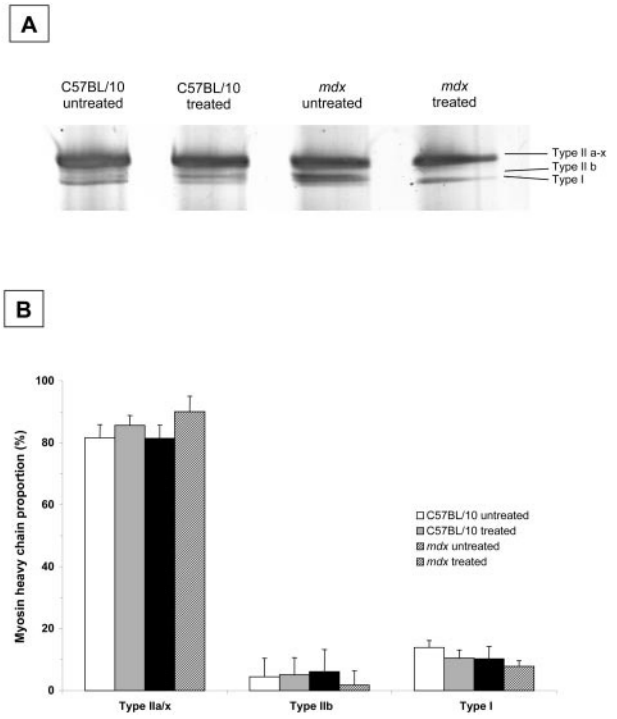

Figure 6. Example gel (**A**) and myosin heavy chain (MyHC) (**B**) proportions in the diaphragm muscles of treated and untreated C57BL/10 and *mdx* mice. Type IIa and IIx MyHC isoforms were grouped together because of their close proximity on the gel. There were no differences in MyHC proportions between strain or treatment groups ($n = 7$ muscles in each group).

Effect of IL-15 on Muscle Regeneration after Myotoxic Injury

Functional regeneration was determined at 2, 6, and 10 days after myotoxic injury. The mass of injured muscles from IL-15-treated mice (8.7 ± 0.2 mg) was ~13% lower than injured muscles from untreated mice (7.6 ± 0.1 mg, $P < 0.05$) at 10 days but not at any other time point. There was no difference in P_o or sP_o for muscles from treated or untreated mice (Table 2).

Box-and-whisker plots representing the distribution of fiber CSAs within injured and uninjured EDL muscles from untreated and IL-15-treated mice are shown in Figure 8. Median fiber CSA in uninjured muscles from untreated mice (688 to 815 μm^2, $n = 3123$ fibers, 95% confidence intervals of median) was greater than in injured muscles from untreated mice (735 to 815 μm^2, $n = 899$). Median fiber CSA in uninjured muscles from IL-15-treated mice was higher after 2 days (900 to 969 μm^2, $n = 735$ fibers) and 6 days (815 to 859 μm^2, $n = 1508$ fibers), but not 10 days (656 to 704, $n = 904$ fibers) after myotoxic injury. Median fiber CSA in injured muscles from untreated mice ranged from 644 to 708 μm^2 ($n = 675$ fibers) at 2 days after injury, 211 to 230 μm^2 ($n = 1439$ fibers) at 6 days after injury, and 504 to 551 μm^2 ($n = 1188$ fibers) at 10 days after injury. Median fiber CSA in injured muscles from IL-15-treated mice was 767 to 857 μm^2 ($n = 854$ fibers) at 2 days after injury, 365 to 410 μm^2 ($n = 1442$ fibers) at 6 days after injury, and 578 to

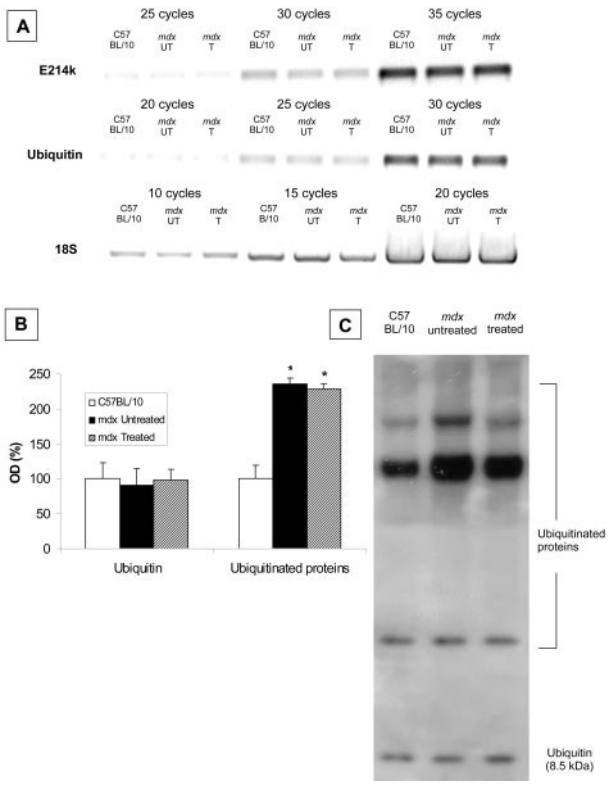

Figure 7. Protein ubiquitination and expression of ubiquitin and ubiquitin-conjugating enzyme E214k/HR6B in diaphragm muscles from IL-15-treated (T) and untreated (UT) C57BL/10 and *mdx* mice. **A:** RT-PCR of ubiquitin and the ubiquitin-conjugating enzyme E214k/HR6B. **B:** Relative levels [ie, when expressed as a percentage of the optical density (OD) for diaphragm muscles from untreated C57/BL10 mice]. **C:** An example gel of ubiquitin and ubiquitinated proteins in diaphragm muscles from IL-15-treated and untreated C57BL/10 and *mdx* mice. Free ubiquitin was detected at a mass of 8.5 kd and several higher molecular weight ubiquitinated proteins were evident. Diaphragm muscles from both treated and untreated *mdx* mice contained higher levels of ubiquitinated proteins compared with diaphragm muscles from C57/BL10 mice ($P < 0.05$, $n = 3$ per group).

633 μm^2 ($n = 1073$ fibers) at 10 days after injury. There was no difference in the proportion of centrally nucleated fibers in the regenerating muscles of treated and untreated mice at any time point.

Discussion

In this study, 4 weeks of IL-15 administration significantly improved the function of, and reduced fibrosis and collagen within, diaphragm muscles of *mdx* mice. Further investigation revealed that IL-15 treatment had a minor anabolic effect on muscle fibers (from limb muscles) during the early period of regeneration after myotoxic injury, similar to its reported mechanism of action on cultured muscle cells *in vitro*. IL-15 treatment did not enhance functional recovery after myotoxic injury. The findings support the contention that administration of IL-15 may have therapeutic potential for muscular dystrophy and other muscle wasting disorders.

The deficits in the functional properties of diaphragm muscles between dystrophic *mdx* and wild-type mice reported in the present study are comparable with those that we have reported previously.[7,8,10,11,18] Although IL-15 treatment had no effect on sP_o of diaphragm muscle strips in wild-type mice, the ~21% improvement in sP_o of the diaphragm of treated compared with untreated *mdx* mice indicates that IL-15 has different effects on normal and dystrophic muscle. Despite the improved sP_o of treated *mdx* mice, there was still an ~32% deficit in functional capacity compared to wild type, demonstrating that IL-15 alone, is not sufficient to ameliorate the dystrophic pathophysiology completely. MyHC isoform composition in the diaphragm muscles of wild-type and *mdx* mice was not affected by IL-15 treatment and so the higher sP_o in IL-15-treated *mdx* mice was not associated with any shift toward a greater proportion of fast (particularly IIB) MyHC isoforms. The lack of any change in diaphragm muscle fatigability provides further evidence that IL-15 did not affect muscle metabolic properties or MyHC isoform composition.

In addition to the improved functional properties of *mdx* diaphragm muscles, there was 24% less collagen infiltration in these muscle strips compared with those from untreated *mdx* mice. Inflammatory cells play a pivotal role in the degeneration of muscle fibers and macrophages, in particular, they coordinate the reconstitution of muscle fibers after degeneration.[43] The greater mac-

Table 2. Contractile and Morphological Properties of Injured and Uninjured EDL Muscles of IL-15-Treated and Untreated C57BL/10 Mice at 2, 6, and 10 Days after Injury

	Untreated		Treated	
	Uninjured	Injured	Uninjured	Injured
2 Days				
Muscle mass (mg)	8.6 ± 0.1	10.3 ± 0.2	8.4 ± 0.2	10 ± 0.1
P_o (mN)	312 ± 4	109 ± 7*	315 ± 4	128 ± 4*
sP_o ($kN \cdot m^2$)	215 ± 3	65 ± 4*	218 ± 3	75 ± 3*
6 Days				
Muscle mass (mg)	8.4 ± 0.1	6.9 ± 0.3	8.4 ± 0.4	7.2 ± 0.3
P_o (mN)	322 ± 9	173 ± 22*	306 ± 14	165 ± 18*
sP_o ($kN \cdot m^2$)	222 ± 6	140 ± 13*	207 ± 5	139 ± 11*
10 Days				
Muscle mass (mg)	9.9 ± 0.5	8.7 ± 0.2*	8.7 ± 0.2	7.6 ± 0.1*
P_o (mN)	355 ± 17	261 ± 18*	333 ± 11	242 ± 5*
sP_o ($kN \cdot m^2$)	204 ± 5	172 ± 10*	214 ± 6	180 ± 5*

CSA, cross sectional area; I/U, injured/uninjured; P_o, peak tetanic contraction force; sP_o, specific maximum isometric tetanic force.
*Injured versus uninjured ($P < 0.05$), $n = 8$ mice per group.

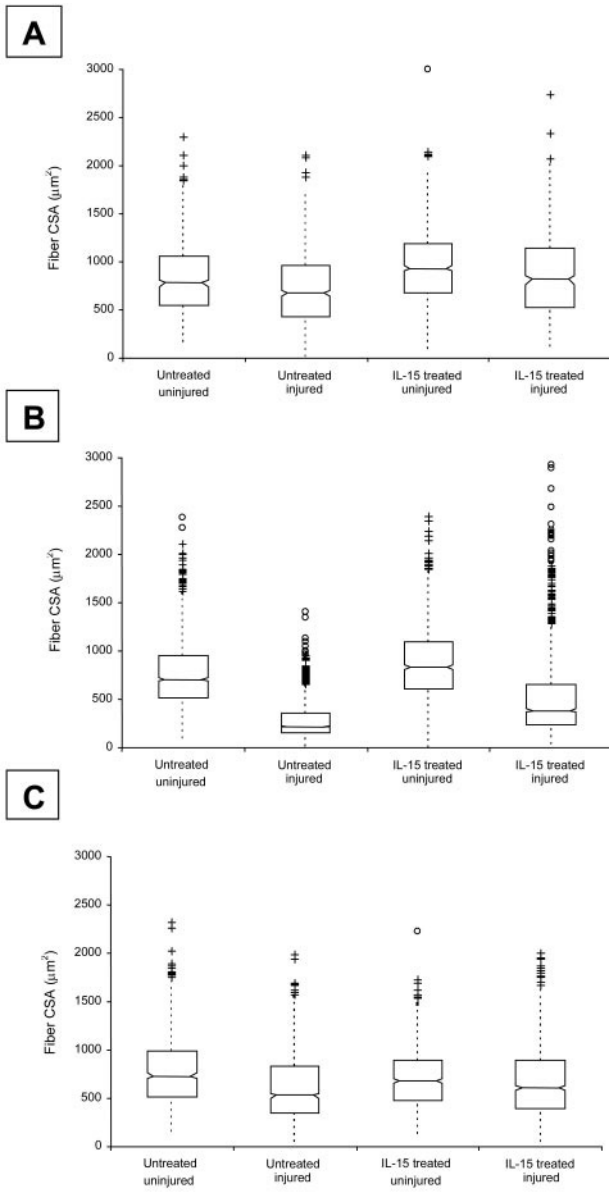

Figure 8. Box-and-whisker plots showing the distribution of fiber CSAs in injured and uninjured EDL muscles from untreated and IL-15-treated C57BL/10 and *mdx* mice, at 2 days (**A**), 6 days (**B**), and 10 days (**C**) after myotoxic injury. Individual outliers are depicted by the cluster of symbols in each case. See text for details.

rophage population, demonstrated by the increased F4/80 reactivity within the diaphragm muscles of *mdx* mice, is consistent with the inflammatory response associated with ongoing muscle degeneration. IL-15 treatment did not affect the macrophage population in the diaphragm muscles of *mdx* mice, indicating that the improvement in the dystrophic pathophysiology was not mediated by an altered inflammatory response. The severity of the dystrophic pathology has been associated with an immune-mediated T-cell-dependent fibrosis[38] and/or myonuclear apoptosis.[37] It has been suggested that immune-based therapies may therefore improve the dystrophic pathology.[44] Whether IL-15 administration may exert an immune-based response has not been determined in dystrophic skeletal muscle. In the present study, we did not observe any change in $CD4^+$ and $CD8^+$ cell numbers after IL-15 treatment. Therefore, our data suggest that possible IL-15-mediated alterations to the T-cell population are not associated with the observed reduction in collagen and improvement in specific force within the *mdx* diaphragm.

Because only a slight increase in median fiber CSA was observed in diaphragm muscles from *mdx* mice after IL-15 treatment, the improvement in functional capacity can likely be attributed to the reduction in collagen infiltration. After intramuscular bupivacaine injection (in limb muscles), IL-15 treatment increased median regenerating fiber CSA at 2 and 6 days, but not 10 days, after injury. Muscle mass and maximum force-producing capacity of regenerating muscles were unaffected, indicating that IL-15 had only limited anabolic effects on skeletal muscle *in vivo*. This is an interesting and novel finding because IL-15 has been shown to increase protein accumulation in myotubes *in vitro*.[27–30]

In another experiment on tumor-bearing rats, IL-15 treatment slowed the rate of muscle wasting associated with cancer, effects attributed to lower expression of components of the ubiquitin-proteasome pathway.[32] We hypothesized that IL-15 treatment may exert similar effects on dystrophic skeletal muscle. It should be noted that cancer cachexia is characterized by an increased rate of proteolysis that leads to rapid loss of muscle protein, whereas muscular dystrophies are typically characterized by a slower and more progressive loss of protein. Our results indicate that gene expression of specific components of the ubiquitin-proteasome pathway (ie, ubiquitin and E214K) and ubiquitin protein levels were not different in diaphragm muscles of *mdx* and C57BL/10 mice, a finding in keeping with previous observations.[45] However, we found that diaphragm muscles of *mdx* mice had higher levels of ubiquitinated proteins compared with C57BL/10 mice. This is likely attributed to the ongoing degeneration and inefficient regeneration in diaphragm muscles of *mdx* mice. IL-15 treatment did not alter the levels of ubiquitinated proteins. It is possible that we did not observe an effect of IL-15 on components of the level of ubiquitinated proteins because unlike cancer cachexia, the rate of muscle wasting in muscular dystrophy is far slower. Our results suggest that the improvement in specific force in diaphragm muscles of IL-15-treated *mdx* mice was therefore not associated with detectable changes in the ubiquitin-proteasome pathway.

Our findings demonstrate that IL-15 administration improved the pathophysiology of dystrophic muscle and highlight a possible therapeutic role for IL-15 in the treatment of neuromuscular disorders especially in which muscle wasting is indicated. Although the precise mechanism by which IL-15 achieves these outcomes is not fully understood, its anabolic effects on regenerating muscle fibers appear relatively minor. Because respiratory insufficiency is a mortality predictor in DMD, any intervention that can ameliorate the dystrophic pathology in the *mdx* diaphragm muscle may have therapeutic potential. Further exploration of the effects of IL-15 on dystrophic skeletal muscle is warranted.

Acknowledgments

We thank Amgen Inc. (Thousand Oaks, CA) for provision of IL-15 and GenMab Inc. (Utrecht, The Netherlands) for provision of the IL-15 antibody.

References

1. Blake DJ, Weir A, Newey SE, Davies KE: Function and genetics of dystrophin and dystrophin-related proteins in muscle. Physiol Rev 2002, 82:291–329
2. Durbeej M, Campbell KP: Muscular dystrophies involving the dystrophin-glycoprotein complex: an overview of current mouse models. Curr Opin Genet Dev 2002, 12:349–361
3. Hoffman EP, Brown RH, Kunkel LM: Dystrophin: the protein product of the Duchenne muscular dystrophy locus. Cell 1987, 51:919–928
4. Ishiura S, Nonaka I, Fujita T, Sugita H: Effect of cyclohexamide administration on bupivacaine-induced acute muscle degeneration. J Biochem 1983, 94:1631–1636
5. Koenig M, Monaco AP, Kunkel LM: The complete sequence of dystrophin predicts a rod-shaped cytoskeletal protein. Cell 1988, 53:219–226
6. Lynch GS, Hinkle RT, Brooks SV, Chamberlain JS, Faulkner JA: Force and power output of fast and slow skeletal muscles from old dystrophic mdx mice. J Physiol Lond 2001, 535:591–600
7. Lynch GS, Rafael JA, Hinkle RT, Cole NM, Chamberlain JS, Faulkner JA: Contractile properties of diaphragm muscle segments from old mdx and old transgenic mdx mice. Am J Physiol 1997, 272:C2063–C2068
8. Dupont-Versteegden EE, McCarter RJ: Differential expression of muscular dystrophy in diaphragm versus hindlimb muscles of mdx mice. Muscle Nerve 1992, 15:1105–1110
9. Louboutin JP, Fichter-Gagnepain V, Thaon E, Fardeau M: Morphometric analysis of mdx diaphragm muscle fibres: comparison with hindlimb muscles. Neuromuscul Disord 1993, 3:463–469
10. Petrof BJ, Stedman HH, Shrager JB, Eby J, Sweeney HL, Kelly AM: Dystrophin protects the sarcolemma from stresses developed during muscle contraction. Am J Physiol 1993, 265:C834–C841
11. Stedman HH, Sweeney HL, Shrager JB, Maguire HC, Panettieri RA, Petrof BJ, Narusawa M, Leferovich JM, Sladky JT, Kelly AM: The mdx mouse diaphragm reproduces the degenerative changes of Duchenne muscular dystrophy. Nature 1991, 352:536–538
12. Khurana TS, Davies KE: Pharmacological strategies for muscular dystrophy. Nat Rev Drug Disc 2003, 2:379–390
13. Cossu G, Sampaolesi M: New therapies for muscular dystrophy: cautious optimism. Trends Mol Med 2004, 10:516–520
14. Muntoni F, Fisher I, Morgan JE, Abraham D: Steroids in Duchenne muscular dystrophy: from clinical trials to genomic research. Neuromuscul Disord 2002, 1:S162–S165
15. Bogdanovich S, Perkins KJ, Krag TOB, Khurana TS: Therapeutics for Duchenne muscular dystrophy: current approaches and future directions. J Mol Med 2004, 82:102–115
16. Barton ER, Morris L, Musaro A, Rosenthal N, Sweeney HL: Muscle-specific expression of insulin-like growth factor I counters muscle decline in mdx mice. J Cell Biol 2002, 157:137–148
17. Fowler EG, Graves MC, Wetzel GT, Spencer MJ: Pilot trial of albuterol in Duchenne and Becker muscular dystrophy. Neurology 2004, 62:1006–1008
18. Gregorevic P, Plant DR, Leeding KS, Bach LA, Lynch GS: Improved contractile function of the mdx dystrophic mouse diaphragm after insulin-like growth factor-I administration. Am J Pathol 2002, 161:2263–2271
19. Lynch GS, Cuffe SA, Plant DR, Gregorevic P: IGF-I treatment improves the functional properties of fast- and slow-twitch skeletal muscles from dystrophic mice. Neuromuscul Disord 2001, 11:260–268
20. Burniston JG, Ng Y, Clark WA, Colyer J, Tan LB, Goldspink DF: Myotoxic effects of clenbuterol in the rat heart and soleus muscle. J Appl Physiol 2002, 93:1824–1832
21. Lynch GS: Update on therapies for sarcopenia: novel approaches for age-related muscle wasting and weakness. Expert Opin Thera Patents 2004, 14:1329–1344
22. Bogdanovich S, Krag TOB, Barton ER, Morris LD, Whittemore LA, Ahima RS, Khurana TS: Functional improvement of dystrophic muscle by myostatin blockade. Nature 2002, 420:418–421
23. Wagner KR, McPherron AC, Winick N, Lee SJ: Loss of myostatin attenuates severity of muscular dystrophy in mdx mice. Ann Neurol 2002, 52:832–836
24. Gregorevic P, Plant DR, Lynch GS: Administration of IGF-I improves fatigue resistance of skeletal muscles from dystrophic mdx mice. Muscle Nerve 2004, 30:295–304
25. Chamberlain JS: Gene therapy of muscular dystrophy. Hum Mol Genet 2002, 11:2355–2362
26. Grabstein KH, Eisenman J, Shanebeck K, Rauch C, Srinivasan S, Fung V, Beers C, Richardson J, Schoenborn MA: Cloning of T cell growth factor that interacts with the beta chain of the interleukin-2 receptor. Science 1994, 264:965–968
27. Quinn LS, Haugk KL, Grabstein KH: Interleukin-15: a novel anabolic cytokine for skeletal muscle. Endocrinology 1995, 136:3669–3672
28. Quinn LS, Anderson BG, Drivdahl RH, Alvarez B, Argiles JM: Overexpression of interleukin-15 induces skeletal muscle hypertrophy in vitro: implications for treatment of muscle wasting disorders. Exp Cell Res 2002, 280:55–61
29. Furmanczyk PS, Quinn LS: Interleukin-15 increases myosin accretion in human skeletal myogenic cultures. Cell Biol Int 2003, 27:845–851
30. Quinn LS, Haugk KL, Damon SE: Interleukin-15 stimulates C2 skeletal myoblast differentiation. Biochem Biophys Res Com 1997, 239:6–10
31. Sakuma K, Watanabe K, Sano M, Uramoto I, Totsuka T: Postnatal profiles of myogenic regulatory factors and the receptors of TGF-β_2, LIF and IGF-I in the gastrocnemius and rectus femoris muscles of dy mouse. Acta Neuropathol 2000, 99:169–176
32. Carbo N, Lopez-Soriano J, Costelli P, Busquets S, Alvarez B, Baccino FM, Quinn LS, Lopez-Soriano FJ, Argiles JM: Interleukin-15 antagonises muscle protein waste in tumour-bearing rats. Br J Cancer 2000, 83:526–531
33. Eisenman J, Ahdieh M, Beers C, Brasel K, Kennedy MK, Le T, Bonnert TP, Paxton RJ, Park LS: Interleukin-15 interactions with interleukin-15 receptor complexes: characterization and species specificity. Cytokine 2002, 20:121–129
34. Vahlsing HL, Varon S, Hagg T, Fass-Holmes B, Dekker A, Manley M, Manthorpe M: An improved device for continuous intraventricular infusions prevents the introduction of pump-derived toxins and increases the effectiveness of NGF treatments. Exp Neurol 1989, 105:233–243
35. Mendez J, Keys A: Density and composition of mammalian muscle. Metabolism 1960, 41:733–743
36. Stupka N, Gregorevic P, Plant DR, Lynch GS: Inhibition of the calcineurin signalling pathway with cyclosporine A impairs muscle regeneration in young mdx mice. Acta Neuropathol 2004, 107:299–310
37. Spencer MJ, Walsh CM, Dorshkind KA, Rodriguez EM, Tidball JG: Myonuclear apoptosis in dystrophic mdx muscle occurs by perforin-mediated cytotoxicity. J Clin Invest 1997, 99:2745–2751
38. Morrison J, Lu QL, Pastoret C, Partridge T, Bou-Gharious G: T-cell-dependent fibrosis in the mdx dystrophic mouse. Lab. Invest 2000, 80:881–891
39. Schertzer JD, Green HJ, Duhamel TA, Tupling AR: Mechanisms underlying increases in SR Ca^{2+}-ATPase activity after exercise in rat skeletal muscle. Am J Physiol 2003, 284:E597–E610
40. Rosenblatt JD, Woods RI: Hypertrophy of rat extensor digitorum longus injected with bupivacaine. A sequential histochemical, immunohistochemical, histological and morphometric study. J Anat 1992, 181:11–27
41. Gregorevic P, Williams DA, Lynch GS: Periodic hyperbaric oxygen exposure enhances contractile function of the regenerating rat soleus muscle following myotoxic injury. Med Sci Sports Exer 2002, 34:630–636
42. Rosenblatt JD: A time course study of the isometric contractile properties of rat extensor digitorum longus muscle injected with bupivacaine. Comp Biochem Physiol 1992, 101A:361–367
43. Wehling M, Spencer MJ Tidball JG: A nitric oxide synthase transgene ameliorates muscular dystrophy in mdx mice. J Cell Biol 2001, 155:123–131
44. Spencer MJ, Montecino-Rodriguez E, Dorshkind K, Tidball JG: Helper ($CD4^+$) and cytotoxic ($CD8^+$) T cells promote the pathology of dystrophin-deficient muscle. Clin Immunol 2001, 98:235–243
45. Combaret L, Taillandier D, Voisin L, Samuels SE, Boespflug-Tanguy O, Attaix D: No alteration in gene expression of components of the ubiquitin-proteasome proteolytic pathway in dystrophin-deficient muscles. FEBS Lett 1996, 393:292–296